

NASA Langley Damage Tolerance Experiences

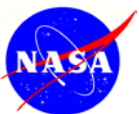
by

Ivatury S. Raju

NASA Engineering and Safety Center
NASA Langley Research Center
Hampton, Virginia

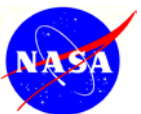
presented at the

**FAA Symposium on
Composite Damage Tolerance
And Maintenance
Chicago
July 19-21, 2006**



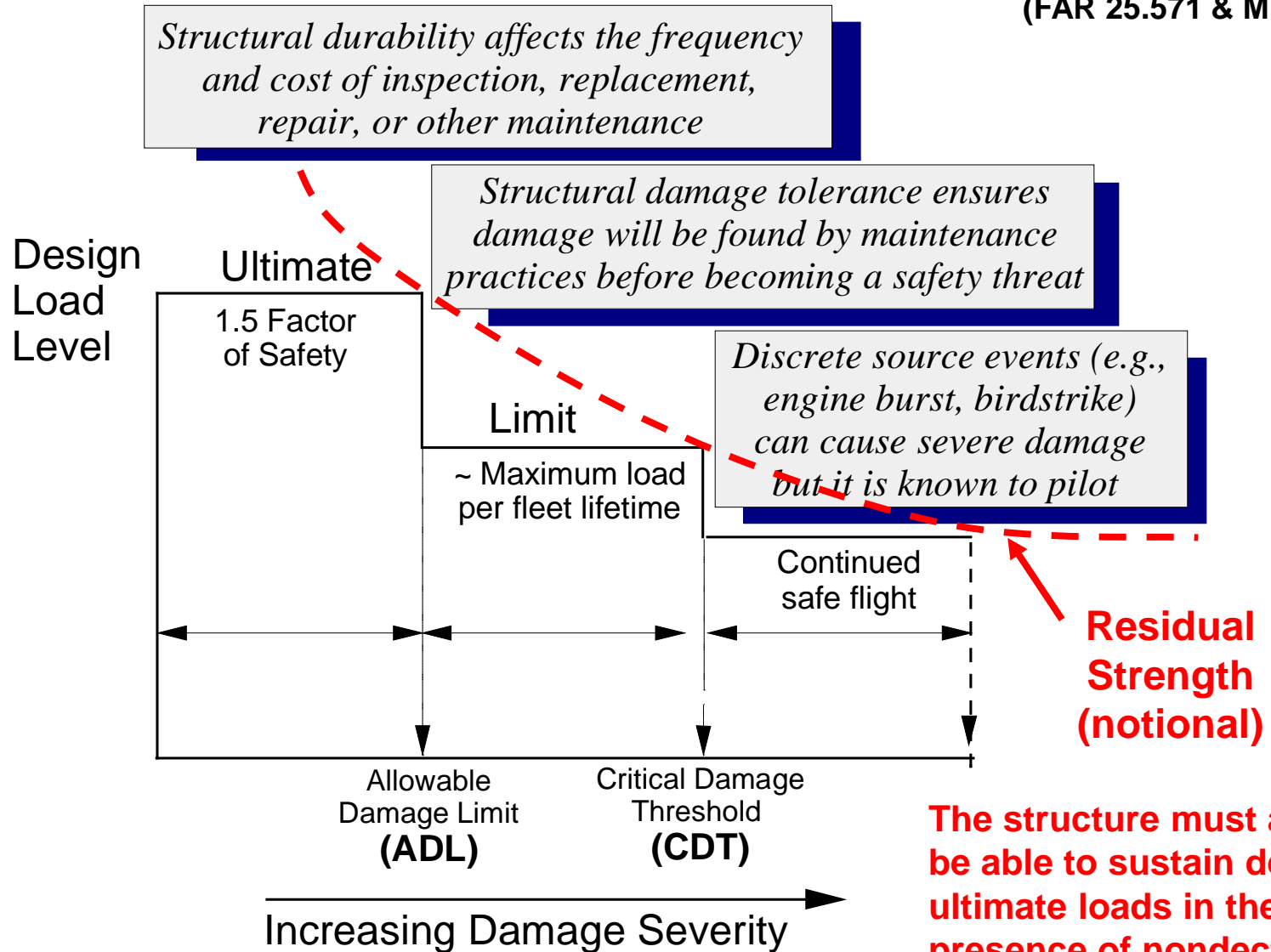
Outline

- NASA Langley's Composites Programs
- SOA Analysis
- Emerging Continuum Methods
- Future Directions

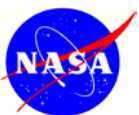


Durability and Damage Tolerance Requirements

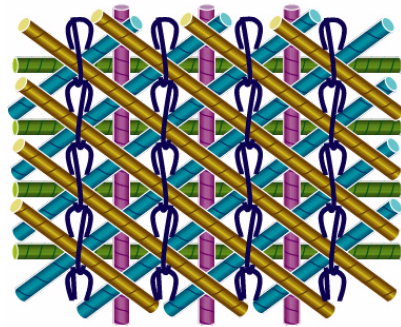
(FAR 25.571 & Mil-17)



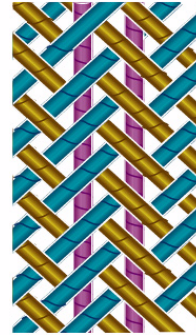
The structure must always be able to sustain design ultimate loads in the presence of non-detectable damage.



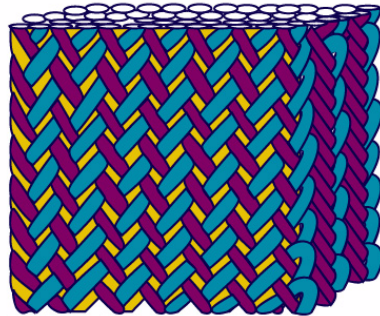
Textile Materials



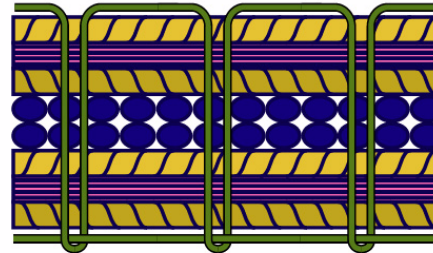
**Multiaxial warp knit
(stitched & unstitched)**



**2-D triaxial braid
(stitched & unstitched)**



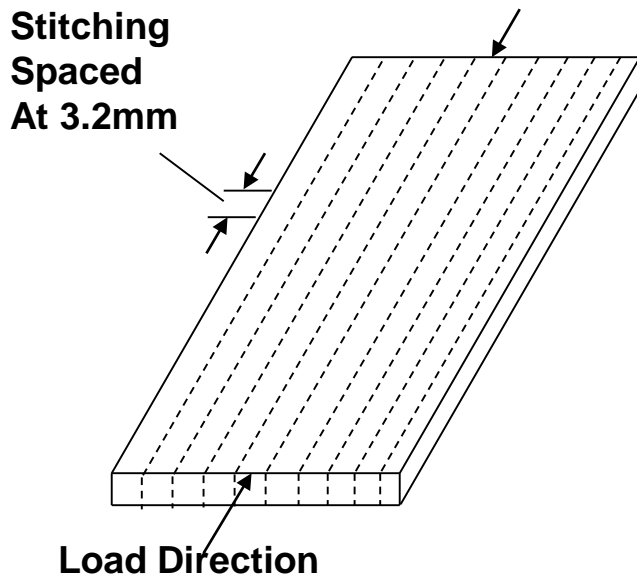
3-D braid



Knitted/stitched

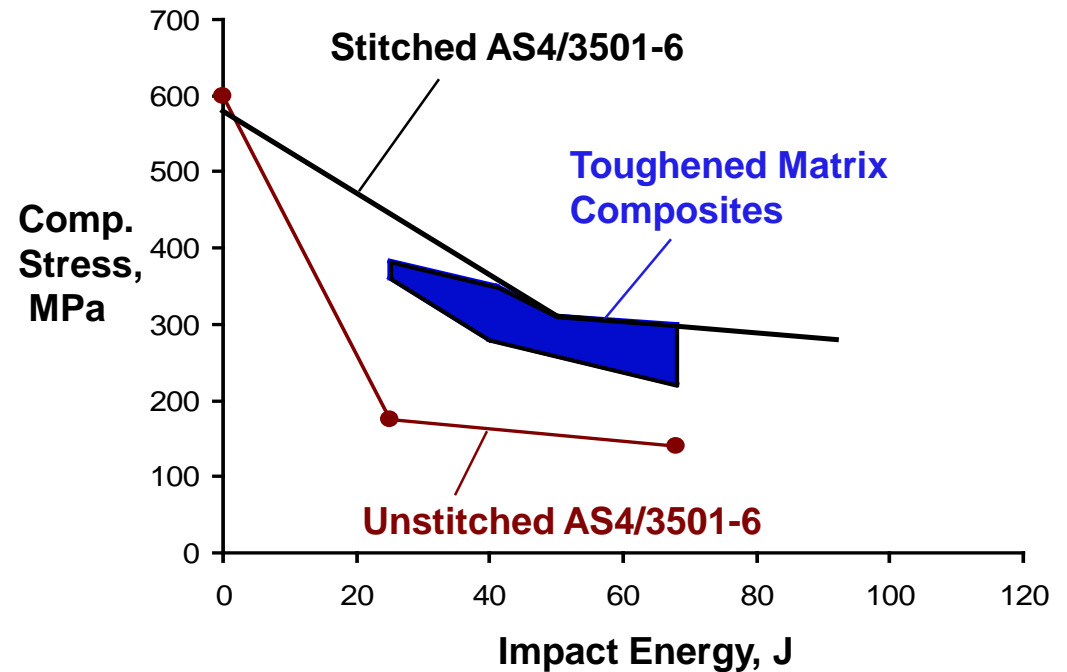
Stitching Improves Damage Tolerance

Details of Stitched Plates

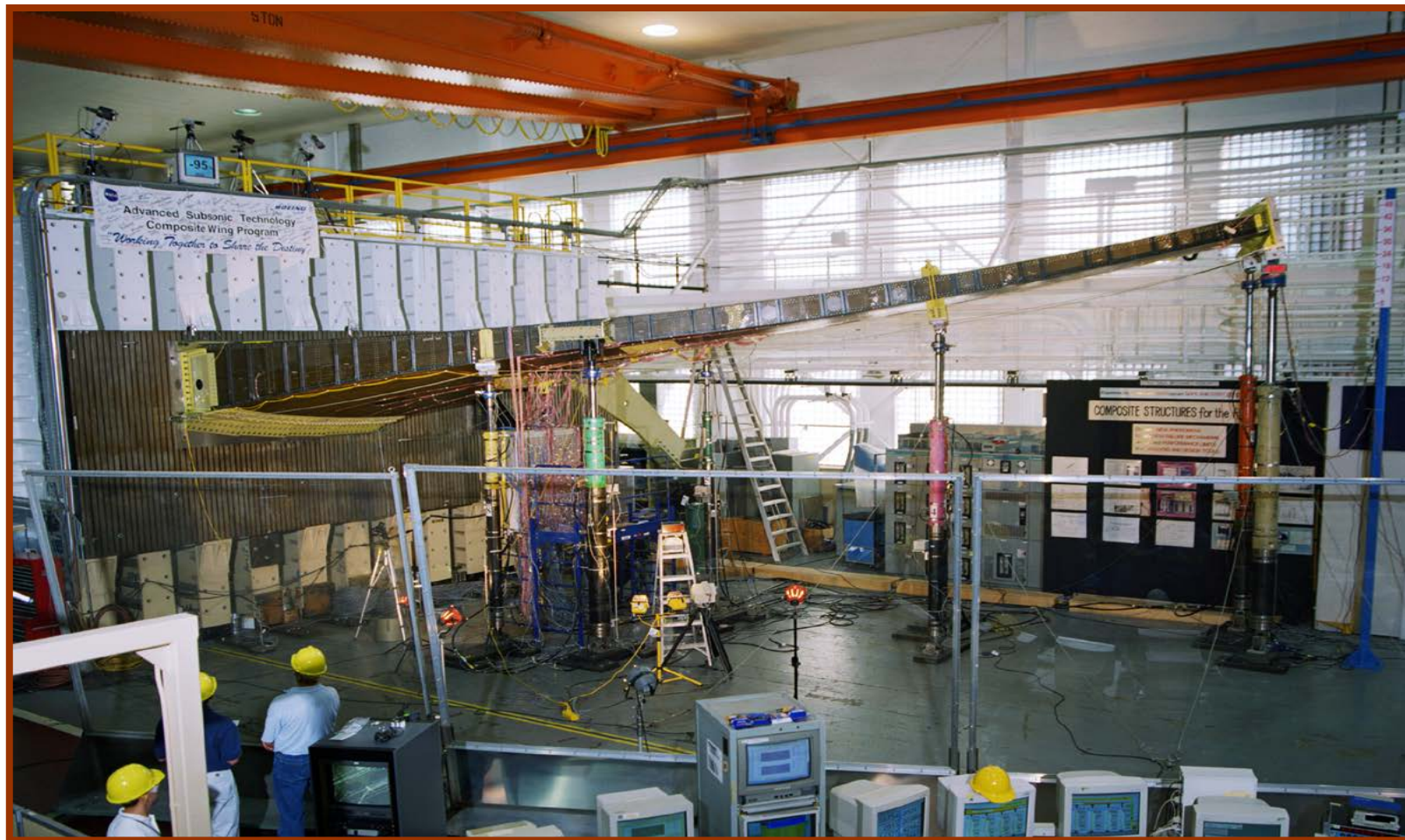


48 ply stitched laminate
[+45/0/-45/90]_{6s}

Compression After Impact Strength

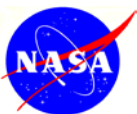


NASA ACT Program – Full Scale Wing Box Test (2000)



AS4/3501-6 and IM7/3501-6 in textile preform

- **No damage or permanent deformation at DLL**
- **Test Article with repair of simulated damage failed at 97% of DUL**



Evolution of Damage Tolerance at NASA Langley (1999-)

Complexity, Computational Expense

Damage Science

Micrographs illustrating damage mechanisms: Stacking Fault, Dislocations, Void Coalescence, and Twinning. Scale bar: 20 μm .

Emerging Continuum Methods

LARC Decohesion Element
(Technology adopted by ABAQUS)

Bilinear Traction-Displacement Law

Mixed-Mode Fracture

FY05 Advances

Delamination growth

Enhanced formulation allows the use of elements up to three times larger than with the classical damage model.

Narrow range

Wide range of element sizes

$$\frac{G_I}{G_c} + (G_{II} - G_{IIc}) \frac{G_{II} + G_{III}}{G_I} + (G_{III} - G_{IIIc}) \frac{G_{III}}{G_I + G_{II}} \frac{G_{II} + G_{III}}{G_I} \geq 1$$

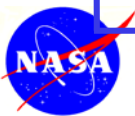
Spin-Offs

Current State-of-the-Art

Graph showing G_I (in-lb/in²) vs Pressure, P (psi). Parameters: $b=0.7570$, $b=0.6250$, $b=0.5000$.

Spin-Offs

Time

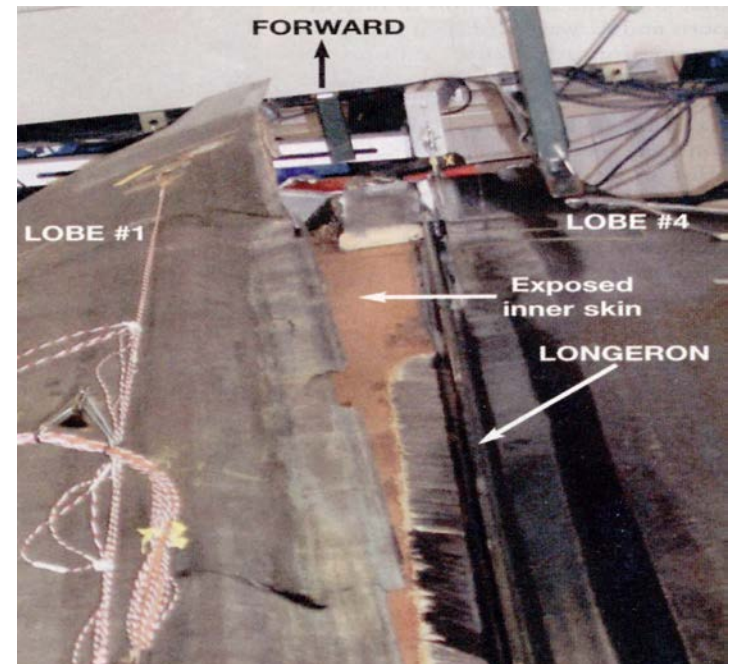
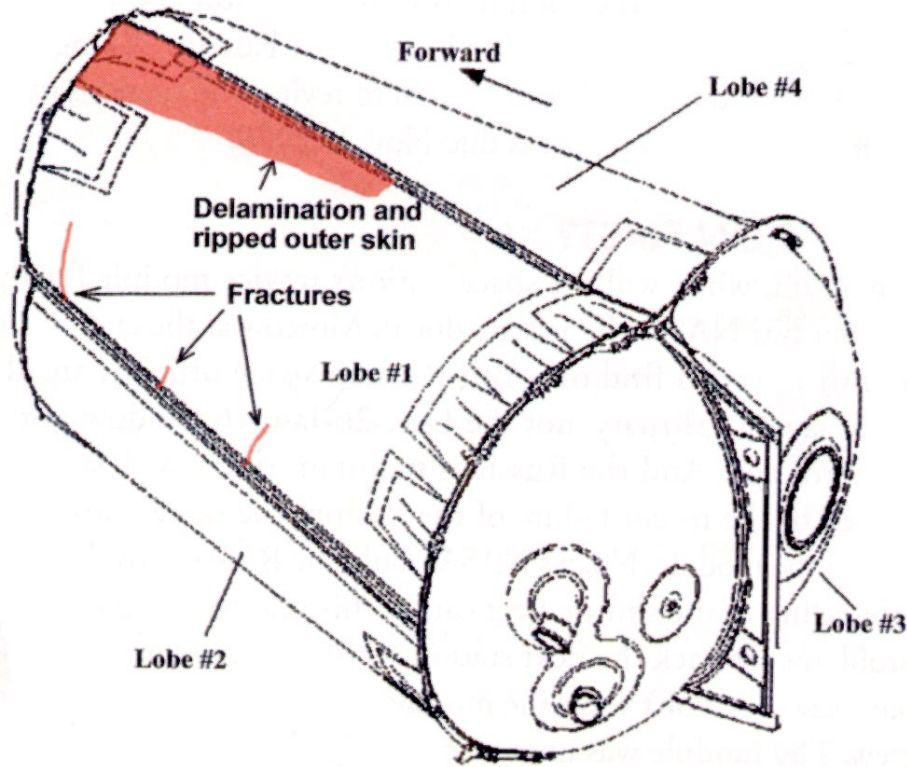


Hypersonic Experimental Vehicle (X-33 Program)

The liquid hydrogen composite tank failed during the protoflight ground test.

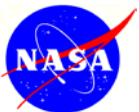
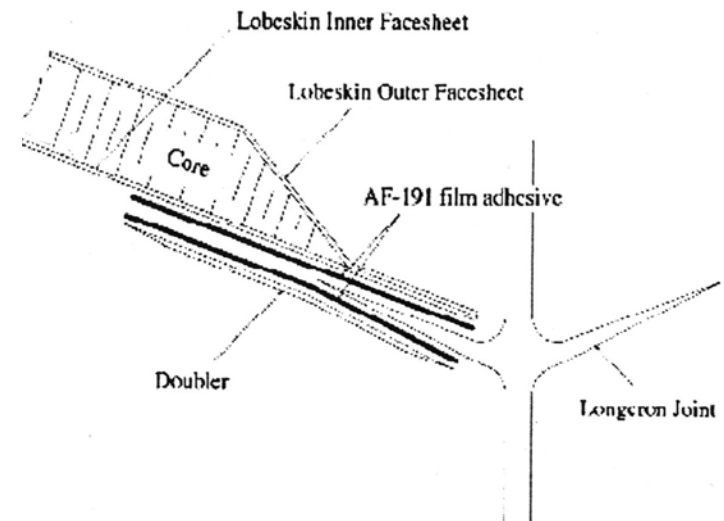


X-33 Composite Liquid Hydrogen Tank Failure

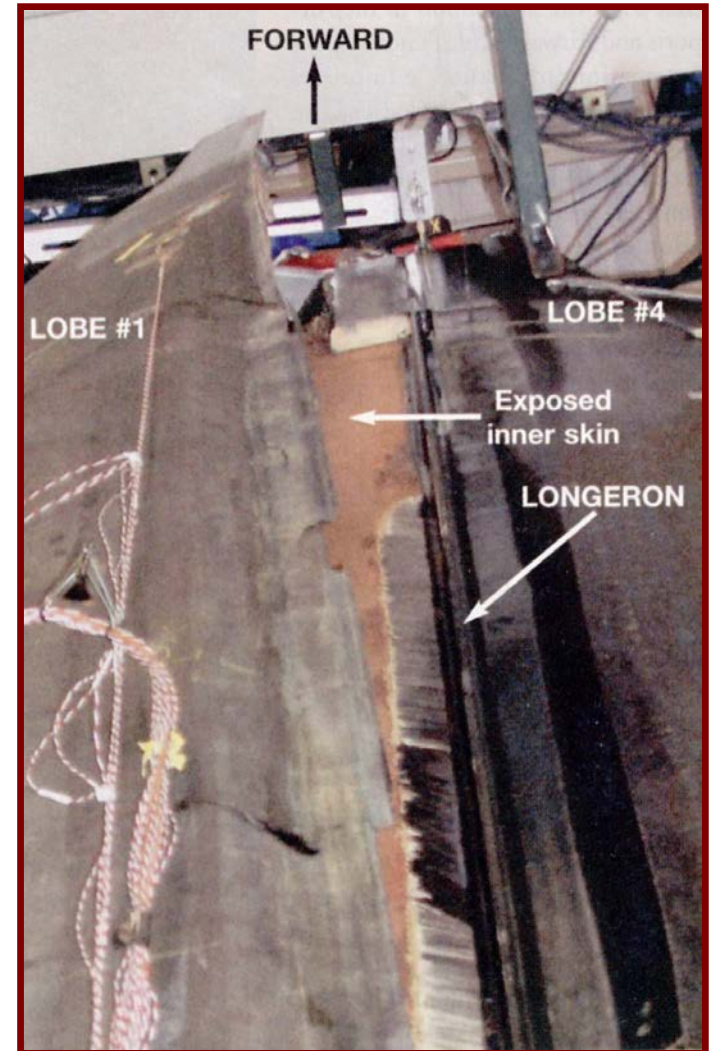
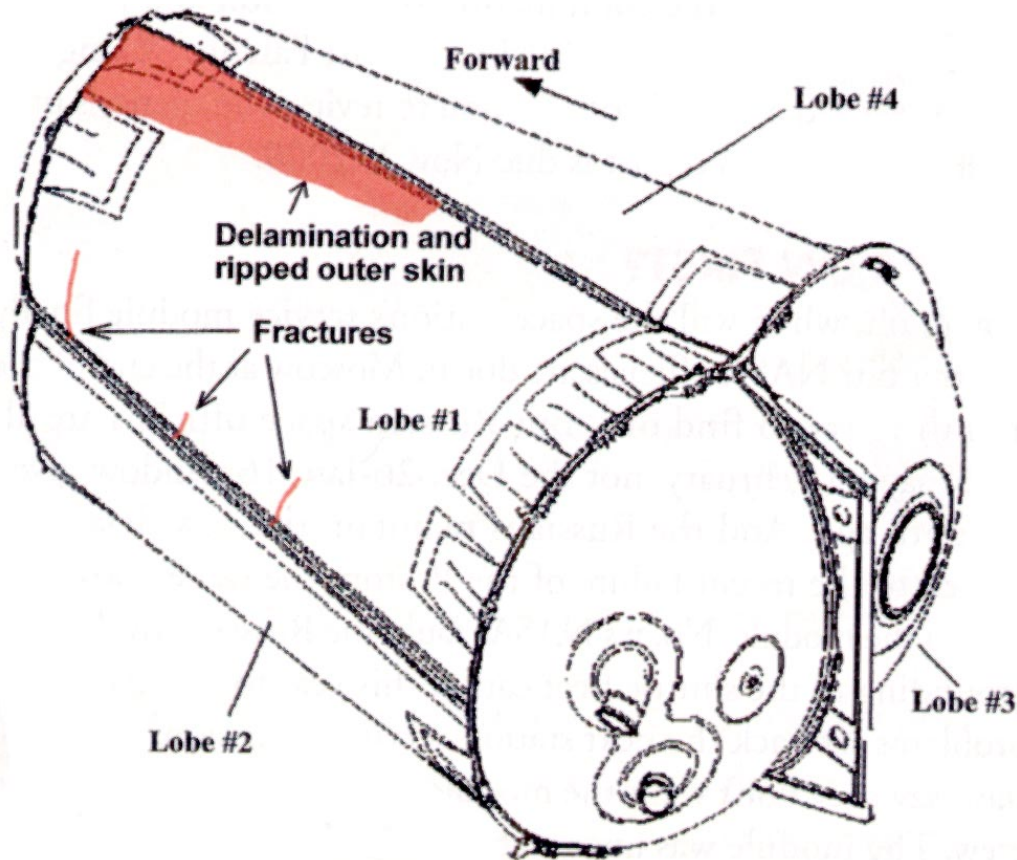


The lobes are sandwich construction:

- The inner face sheet is $[45/90_3/-45/0_3/-45/90_3/45]_T$
- The outer face sheet is $[65/0/-65/90/-65/0/65]_T$
- The face sheets are IM7/977-2 laminates.
- The core is a honeycomb Korex 3/16 - 3.0 (1.5 in. thick).
- The adhesive is AF-191.

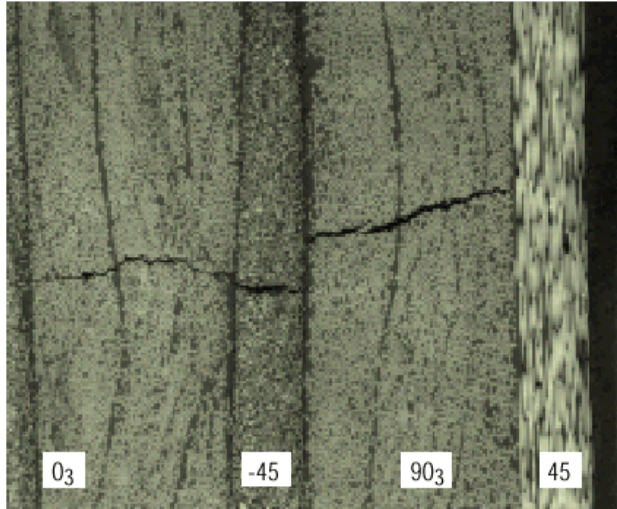


X-33 Composite Liquid Hydrogen Tank Failure



Causes of the X-33 Composite Tank Failure

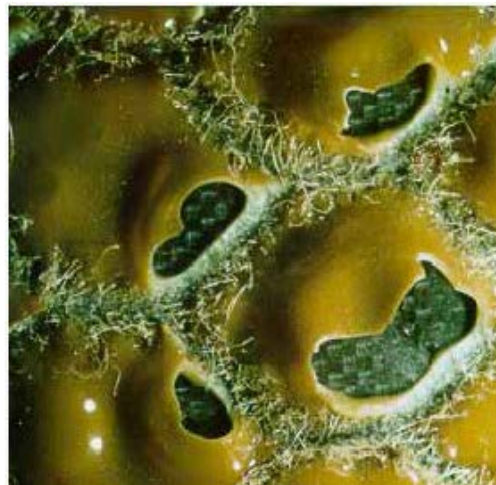
Inner Skin Microcracking



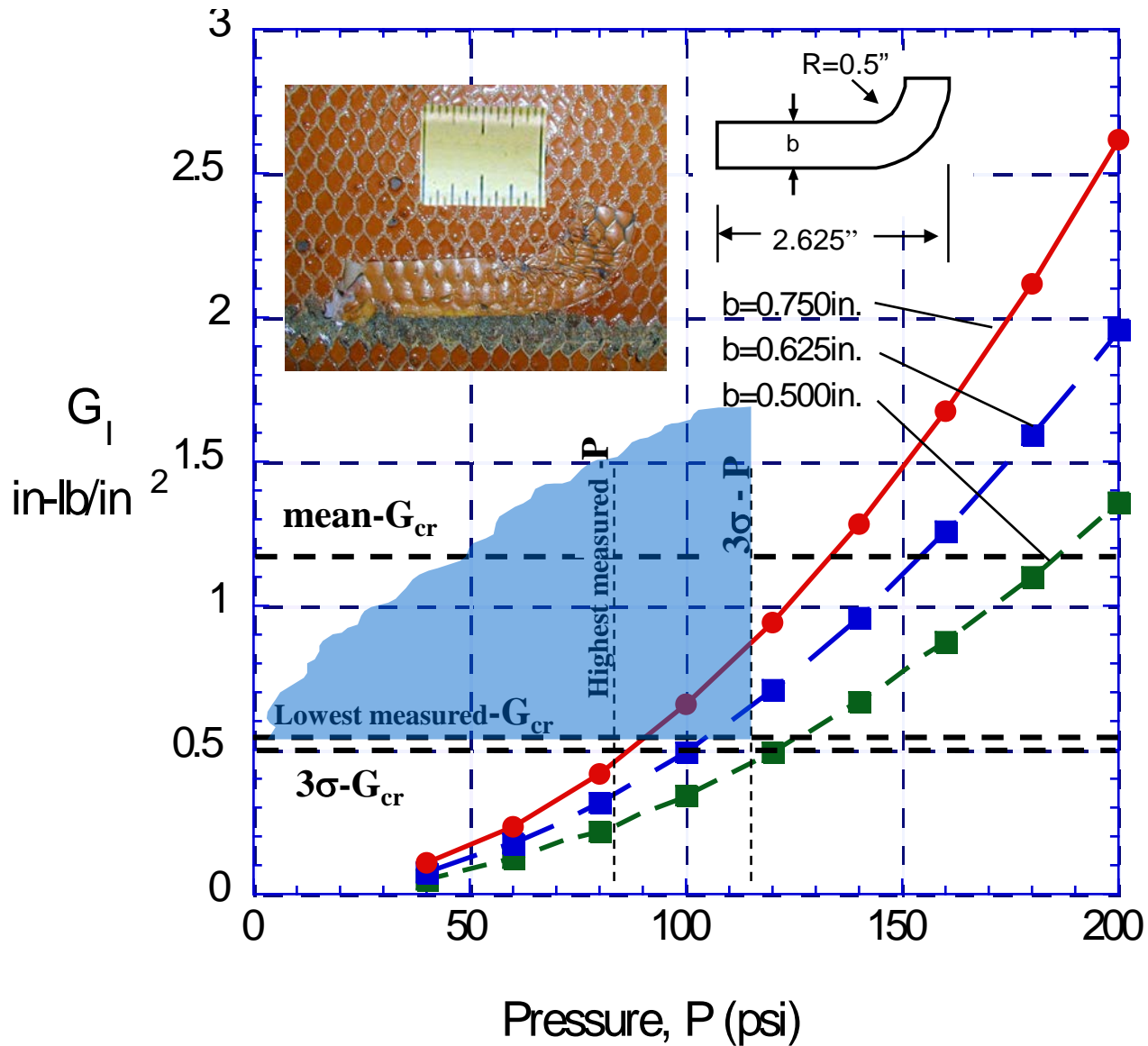
Teflon Tape in Core



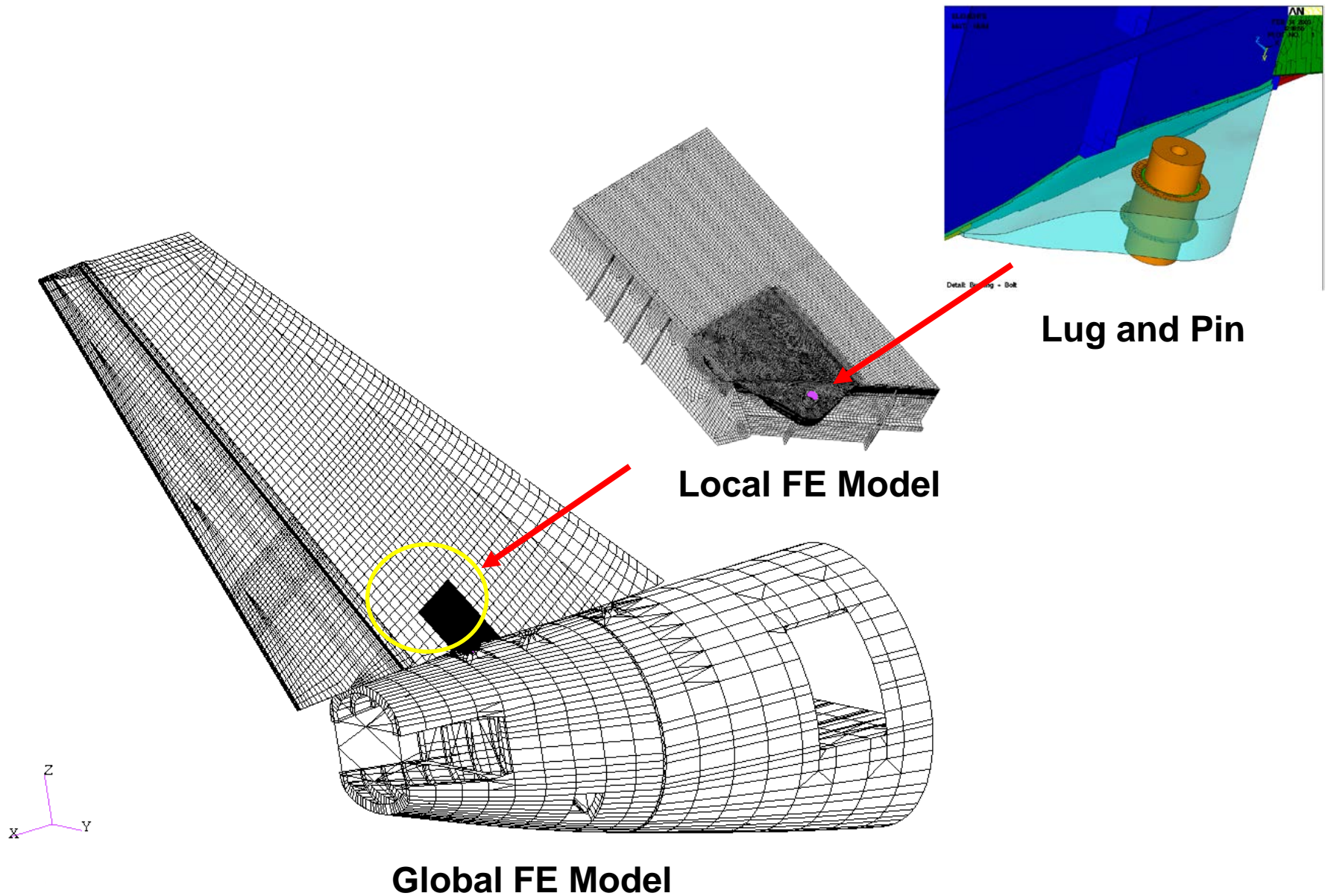
Weak Core to Face Sheet Bond Strength/Toughness



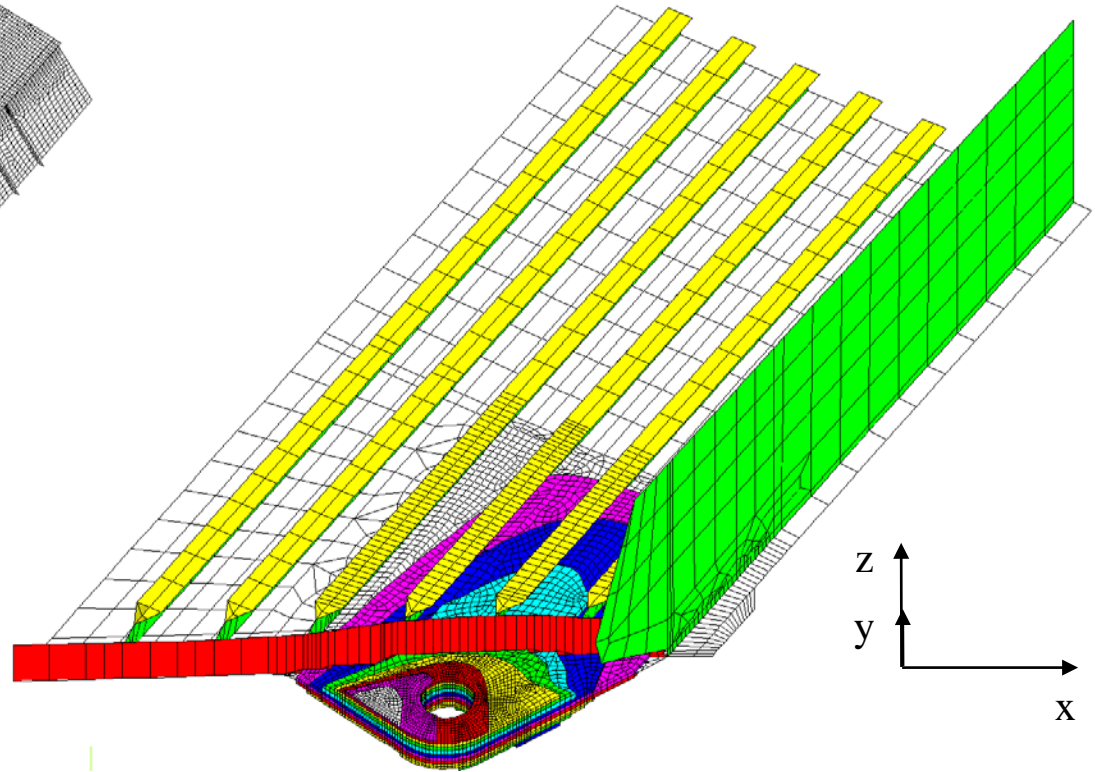
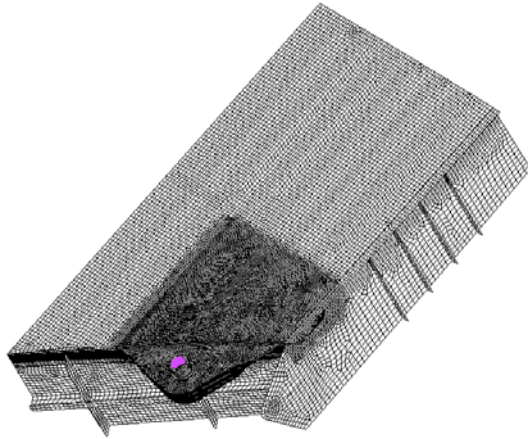
Strain Energy Release Rates for an F.O.D. Debond



Rear Fuselage and Tail Configuration



3D-Shell Finite Element Model



Attributes

25,931 nodes

21,519 elements

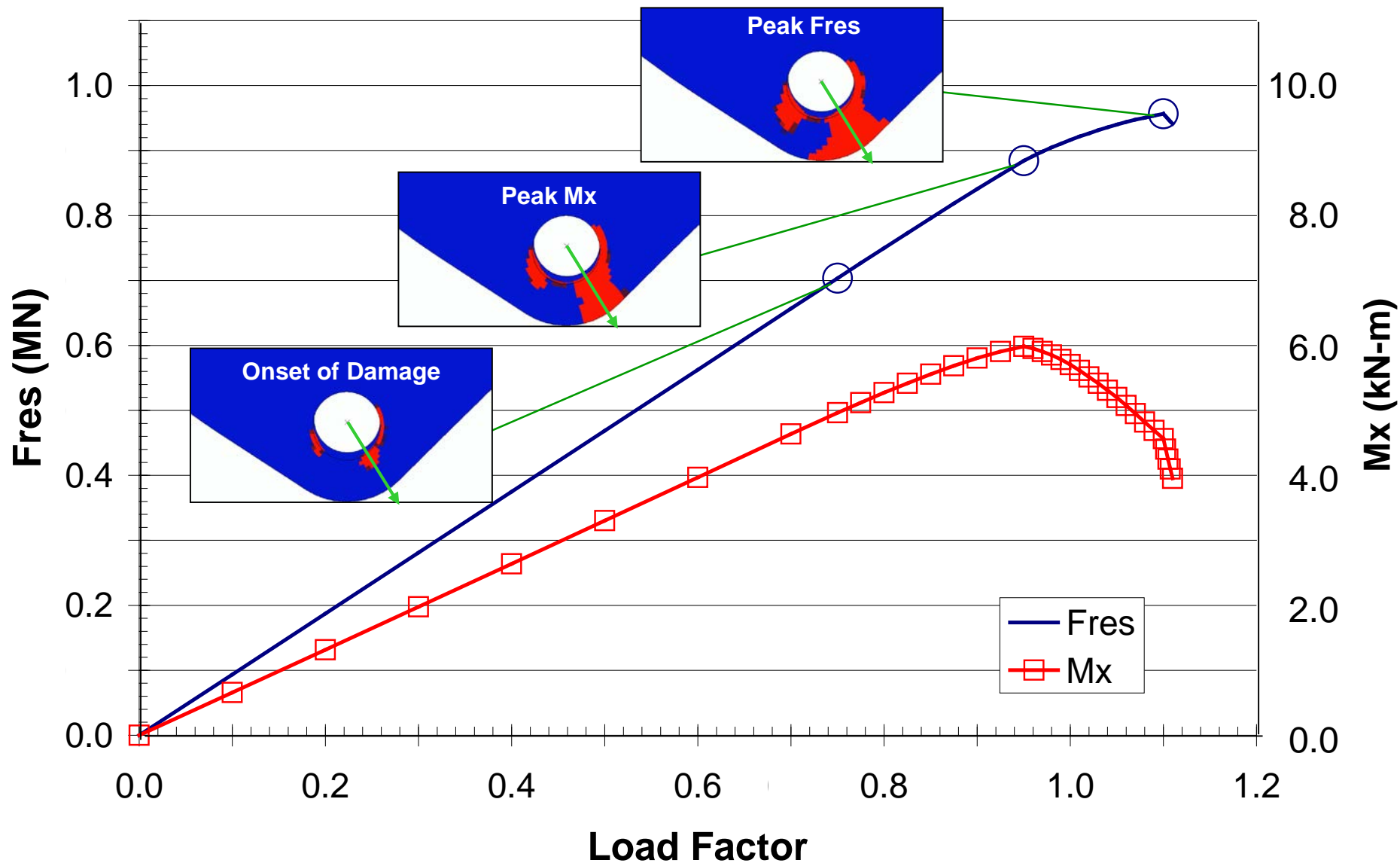
Contact modeled

200 plies in lug

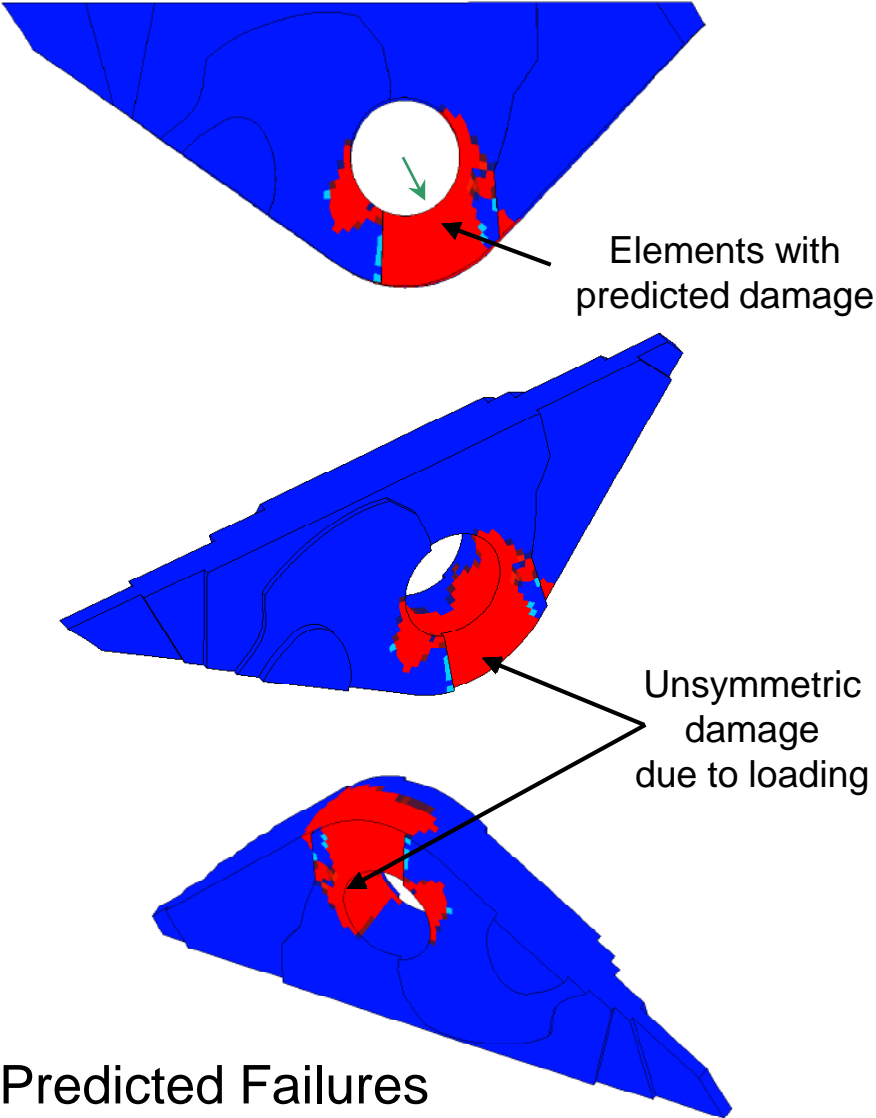
Global-local coupled analysis

Damage monitored as load incremented

Damage Propagation from PFA



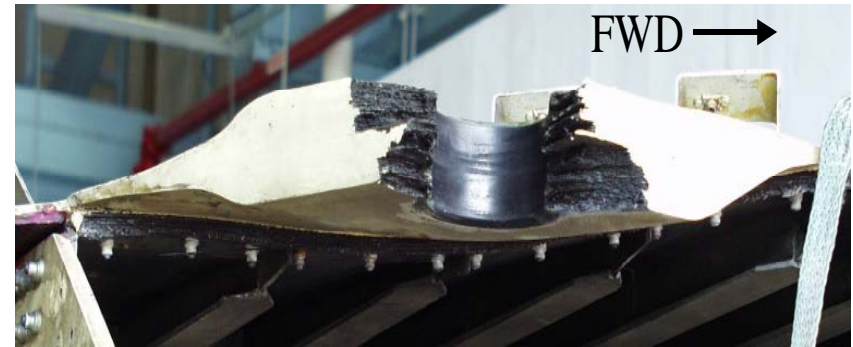
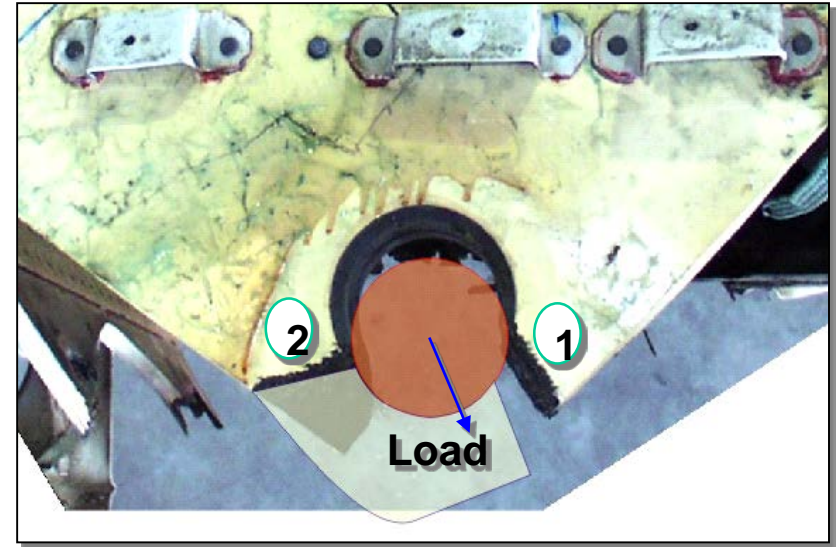
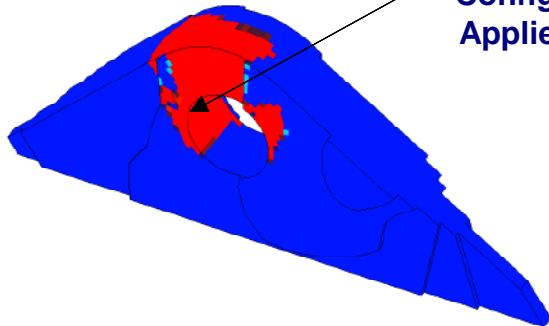
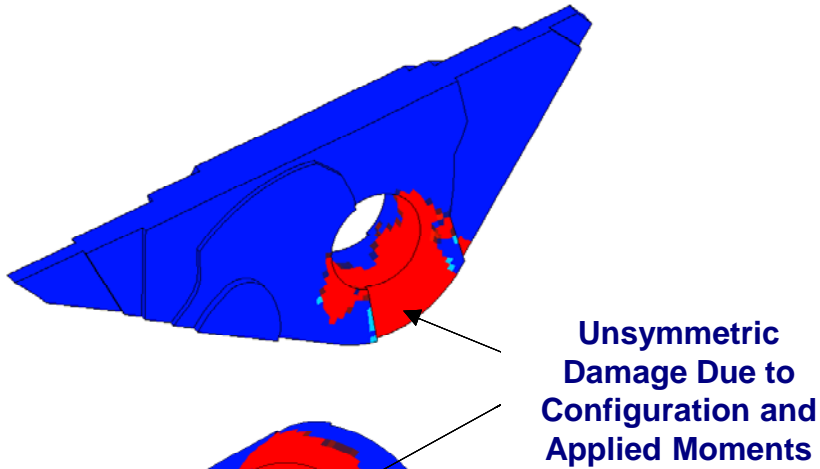
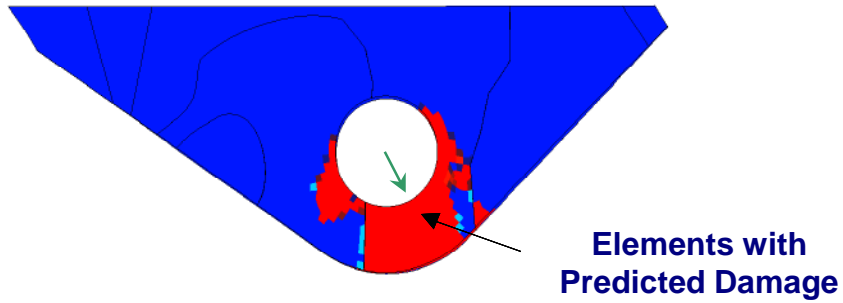
Comparison of Predicted and Test Results



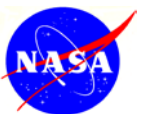
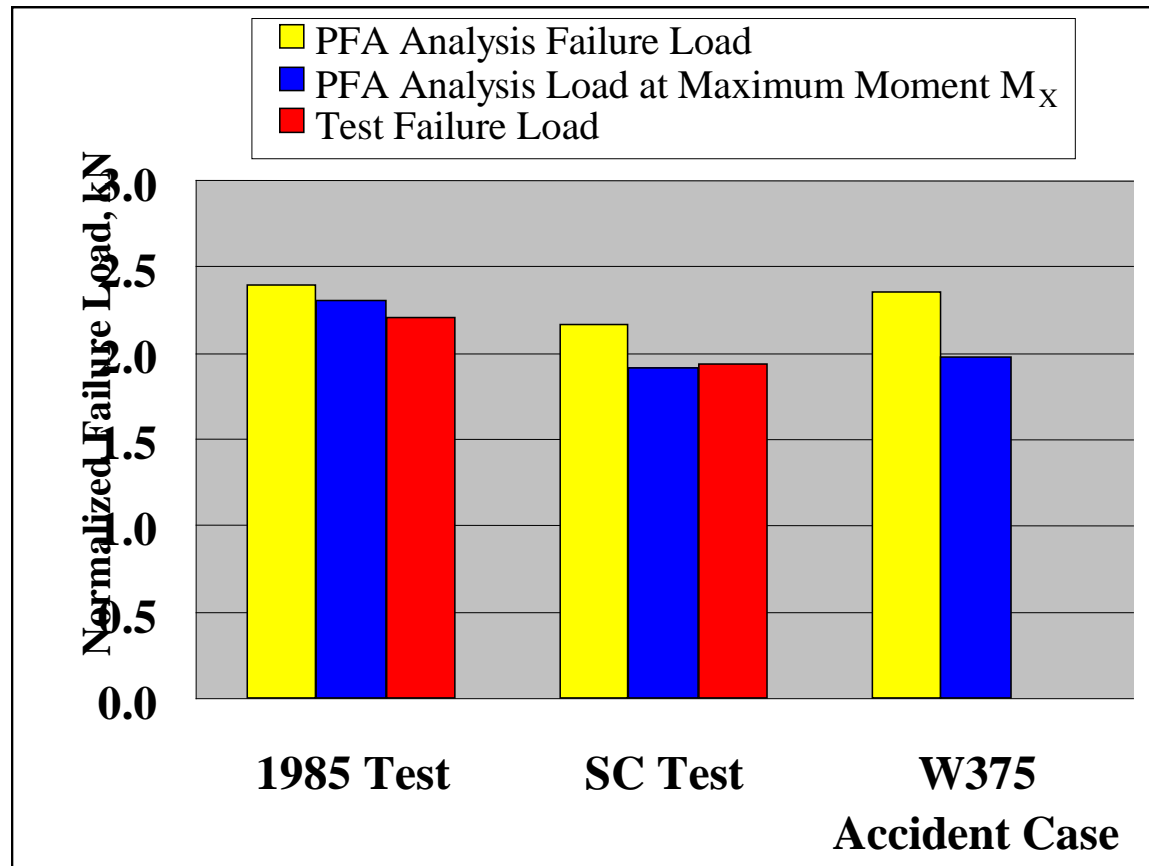
Failed Test Lug

Test Failure Load	907 kN
Predicted Failure Load	896 kN

W375 Accident Conditions – Damage



Normalized Failure Load for 1985-Certification Test, 2003-Subcomponent Test and W375 Accident Condition



Evolution of Damage Tolerance at NASA Langley (1999-)

Complexity, Computational Expense

Damage Science

Micrographs illustrating damage mechanisms: Stacking Fault, Dislocations, Void Coalescence, and Twinning. Scale bar: 20 μm .

Emerging Continuum Methods

LARC Decohesion Element
(Technology adopted by ABAQUS)

Bilinear Traction-Displacement Law

Mixed-Mode Fracture

FY05 Advances

Enhanced formulation allows the use of elements up to three times larger than with the classical damage model.

Narrow range vs Wide range of element sizes.

$$\frac{G_I}{G_c} + (G_{II} - G_{IIc}) \left(\frac{G_{II} + G_{III}}{G_I} \right)^b + (G_{III} - G_{IIIc}) \left(\frac{G_{II} + G_{III}}{G_I} \right)^c \geq 1$$

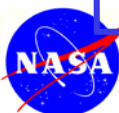
Spin-Offs

Current State-of-the-Art

Graph showing G_I (in-lb/in²) vs Pressure, P (psi). Parameters: $b=0.7510$, $b=0.6250$, $b=0.5000$.

Spin-Offs

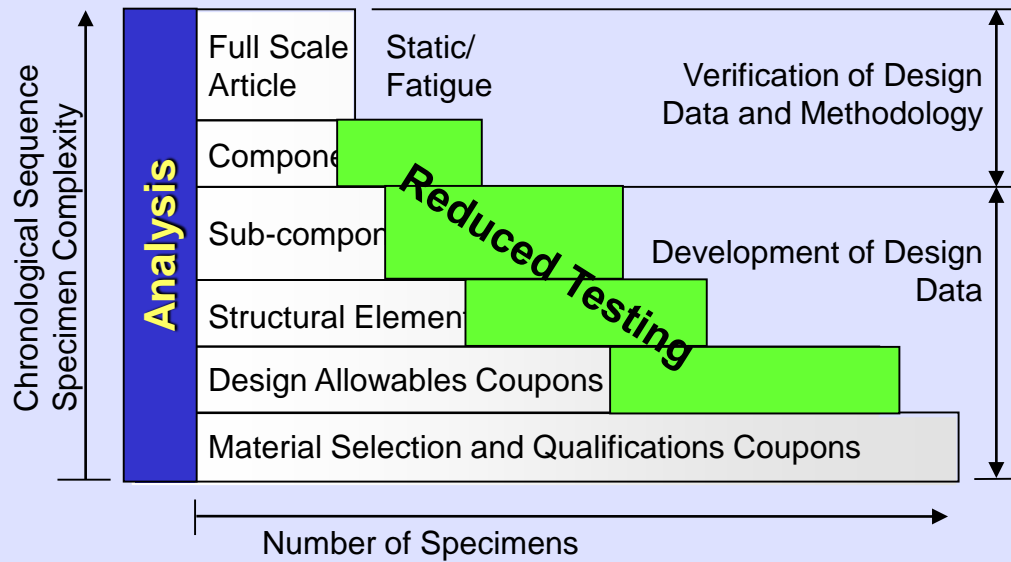
Time



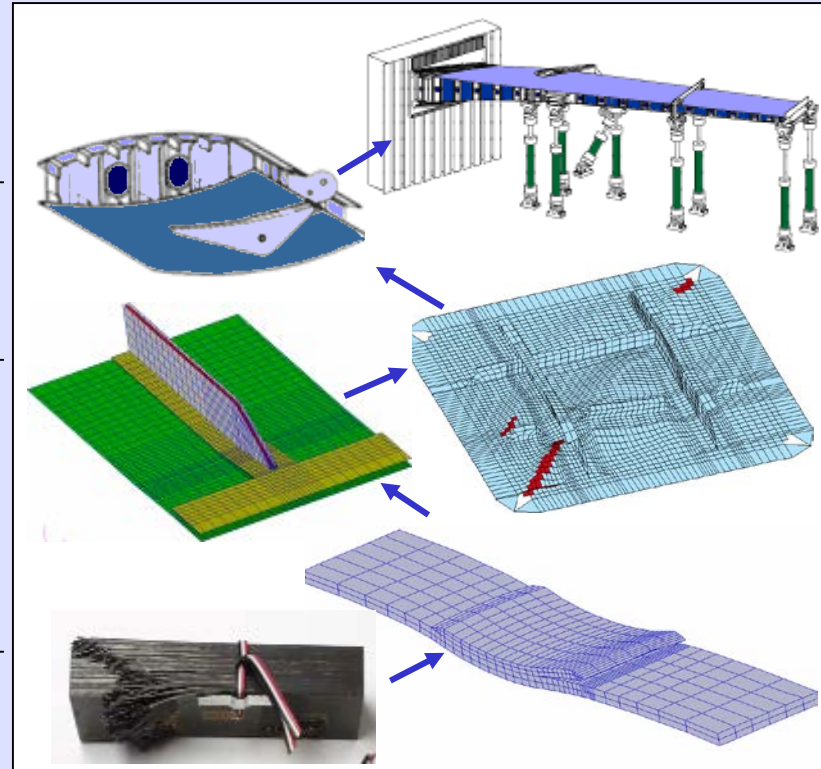
Building Block Approach

Building Block Integration.

Certification Methodology (Mil-Hbk.-17)



Structural Levels of Testing & Analysis



● High-Fidelity Progressive Failure Analysis

- Reduced reliance on testing
- Faster design process

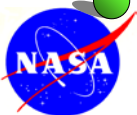


reduced non-recurring costs

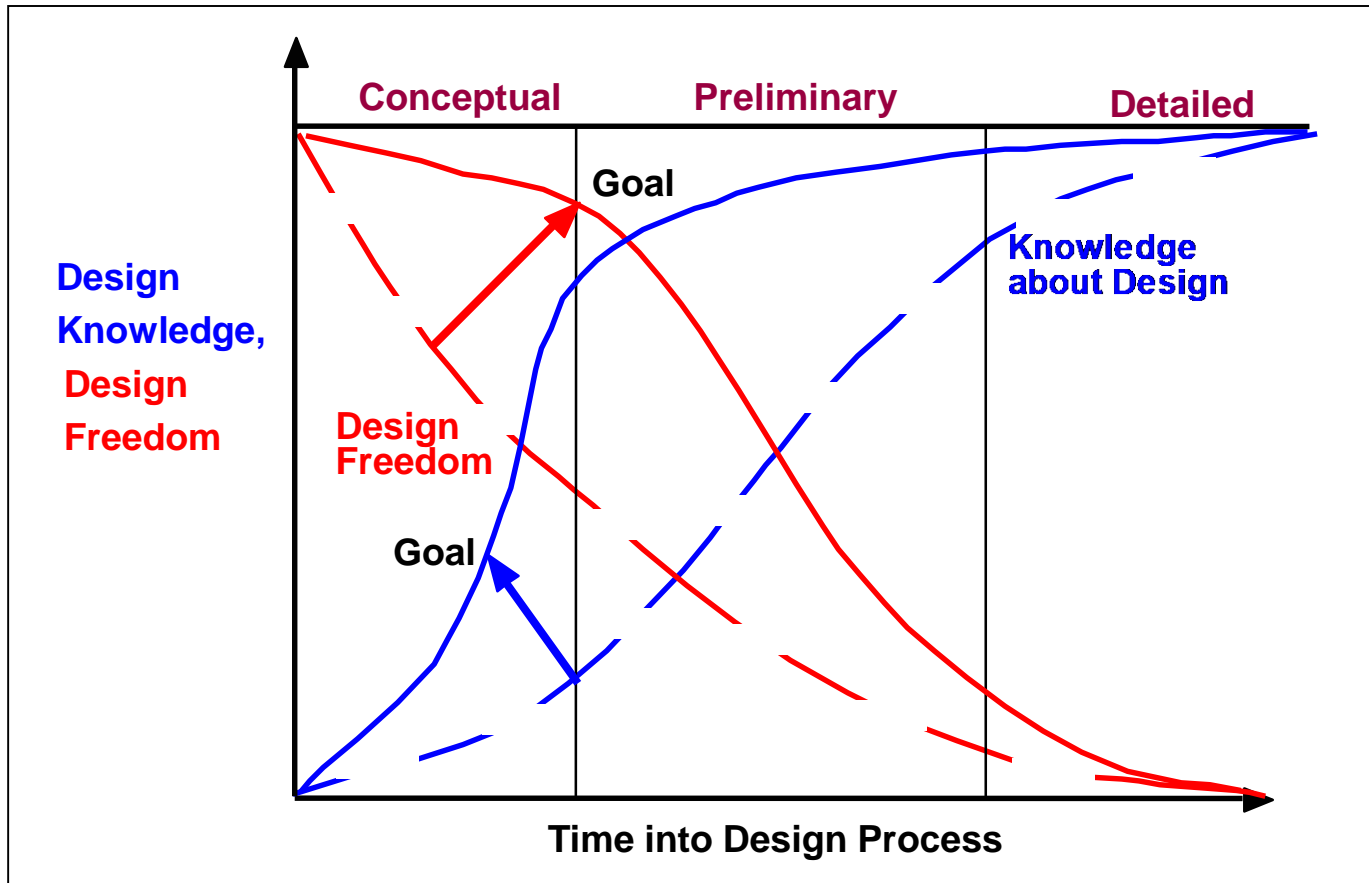
- More accurate design tools



reduced recurring costs



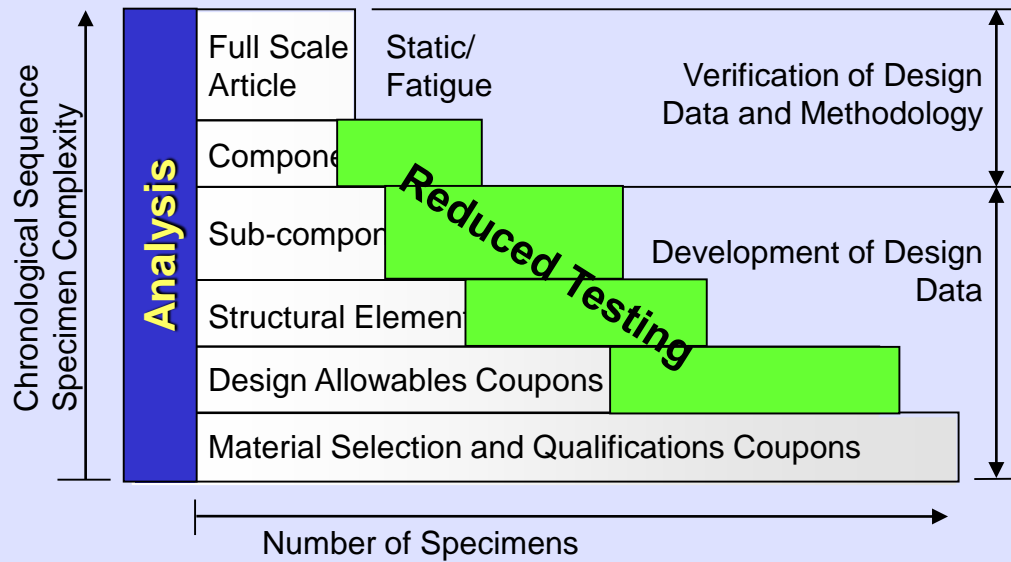
Design Freedom vs. Knowledge



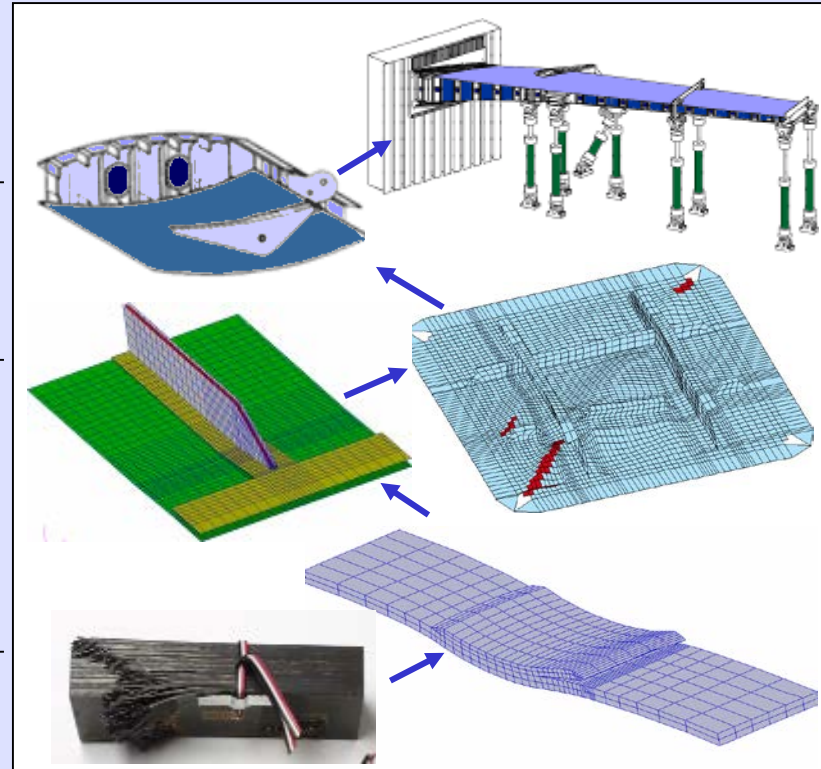
Building Block Approach

Building Block Integration.

Certification Methodology (Mil-Hbk.-17)



Structural Levels of Testing & Analysis



● High-Fidelity Progressive Failure Analysis

- Reduced reliance on testing
- Faster design process

} → reduced non-recurring costs

- More accurate design tools

→ reduced recurring costs

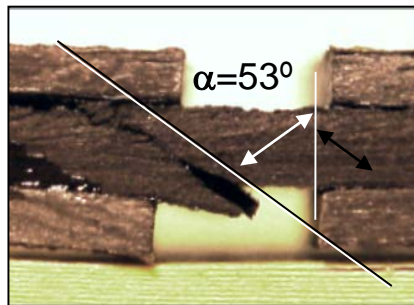
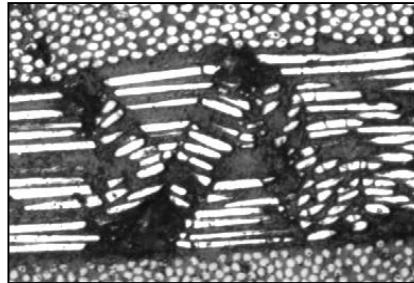
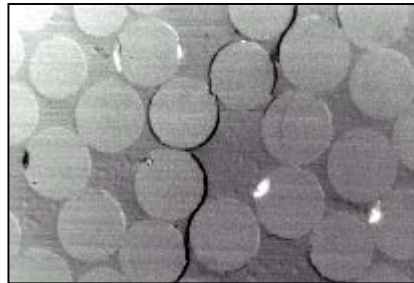


Failure Criteria for Laminated Composites

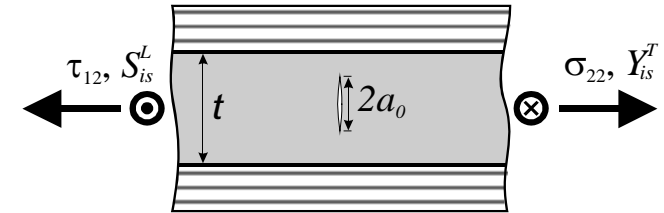
- Failure Criteria are used for predicting damage initiation and final failure
- Composites have multiple damage modes; each requires a different criterion

LaRC04 Criteria

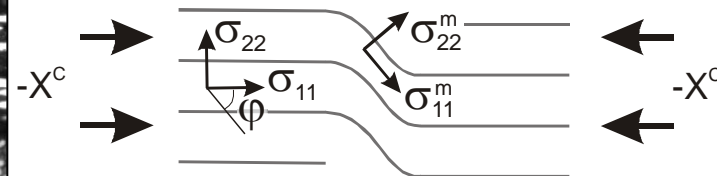
- In-situ matrix strength prediction
- Advanced fiber kinking criterion
- Prediction of angle of fracture (mat. compression)
- Criteria used as activation functions within framework of damage mechanics



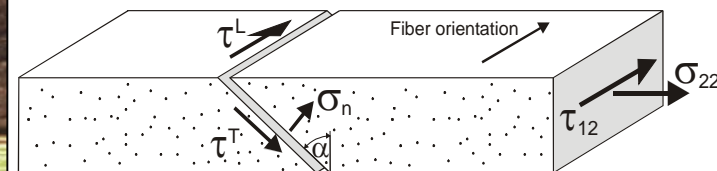
Matrix Tension & Shear



Fiber Compression



Matrix Compression and Shear



LaRC04 in Continuum Damage Model

Gibbs Free Energy

$$G = \frac{1}{2} \sigma : H : \sigma + \sigma : \alpha \Delta T =$$

$$= \frac{\sigma_{11}^2}{2(1-d_1)E_1} + \frac{\sigma_{22}^2}{2(1-d_2)E_2} + \frac{\nu_{12}}{E_1} \sigma_{11} \sigma_{22} + \frac{\sigma_{12}^2}{2(1-d_6)G_{12}} + (\alpha_{11} \sigma_{11} + \alpha_{22} \sigma_{22}) \Delta T$$

Strains: $\varepsilon = \frac{\partial G}{\partial \sigma} = H : \sigma + \alpha \Delta T$

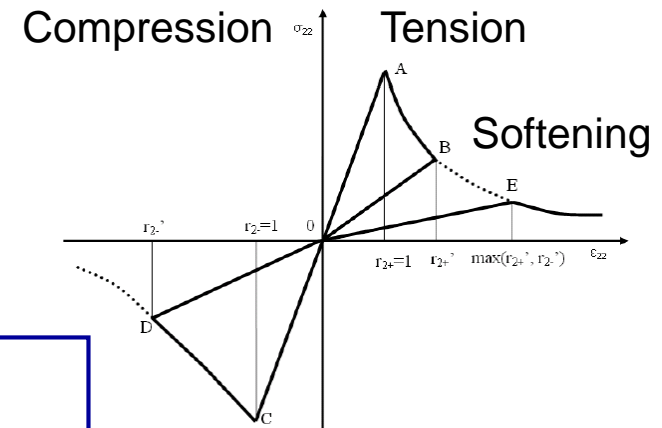
Lamina Secant Relation

$$H = \frac{\partial^2 G}{\partial^2 \sigma} = \begin{bmatrix} \frac{1}{(1-d_1)E_1} & -\frac{\nu_{21}}{E_2} & 0 \\ -\frac{\nu_{12}}{E_1} & \frac{1}{(1-d_2)E_2} & 0 \\ 0 & 0 & \frac{1}{(1-d_6)G_{12}} \end{bmatrix}$$

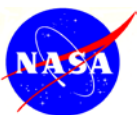
Rate of Damage Growth

$$d_i = 1 - \frac{1}{f_i(r_i)} \exp(A_i(1 - f_i(r_i)))$$

f_i : LaRC04 failure criteria as activation functions



CDM ensures consistent material degradation and mesh-independent solution



Z-Pin Technology

● Definition

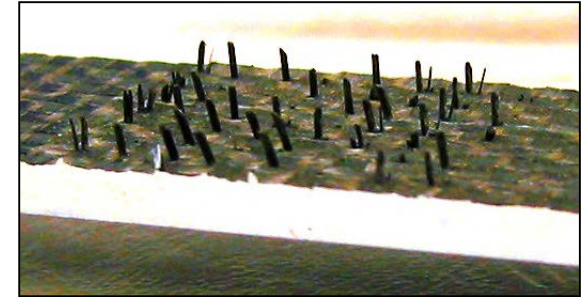
- Pultruded graphite rods positioned through-thickness (z-direction) of a composite laminate
- Pins are 0.2-0.5mm diameter rods
- Typical range of areal density between 0.5% and 4%
- Inserted into uncured laminate using ultrasonic hammer

● Purposes / Drawbacks

- Improve composite laminate transverse strength
- Prohibit delamination
- Degrade laminate (in-plane) properties, see micrograph

● Applications

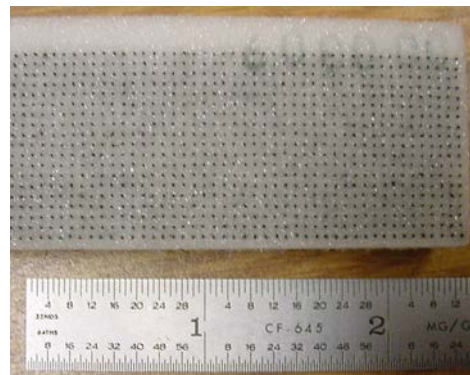
- Areas with significant out-of-plane loads such as bonded stiffener termination
- Areas exposed to impact damage threat



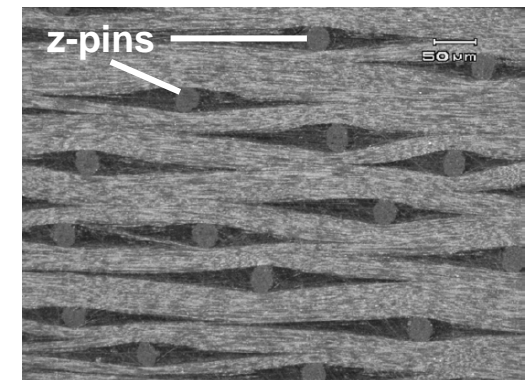
Z-Pins protruding from laminate*



Z-Pin preform: Upper side**

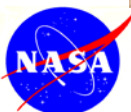


Z-Pin preform: Insertion side**



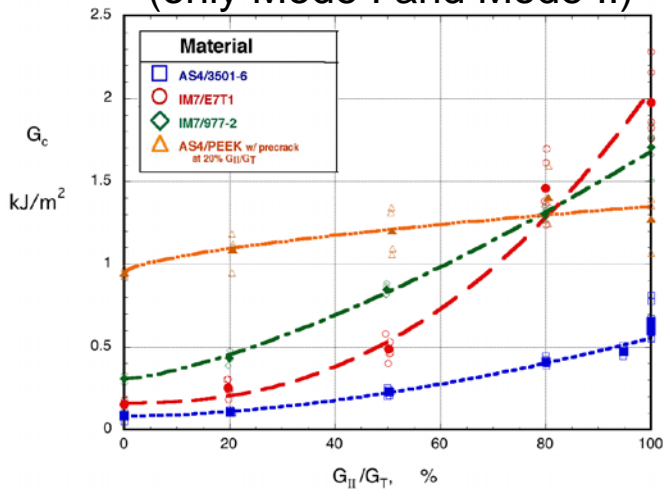
Fiber misalignment from z-pins***

*James Ratcliffe, NIA. **Pierre Minguet, Boeing. ***Jeffery Schaff, Sikorsky Aircraft.



New Delamination Criterion Needed

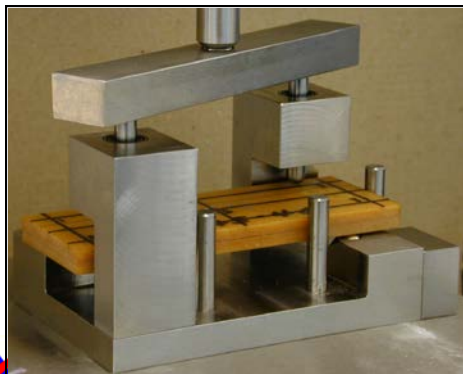
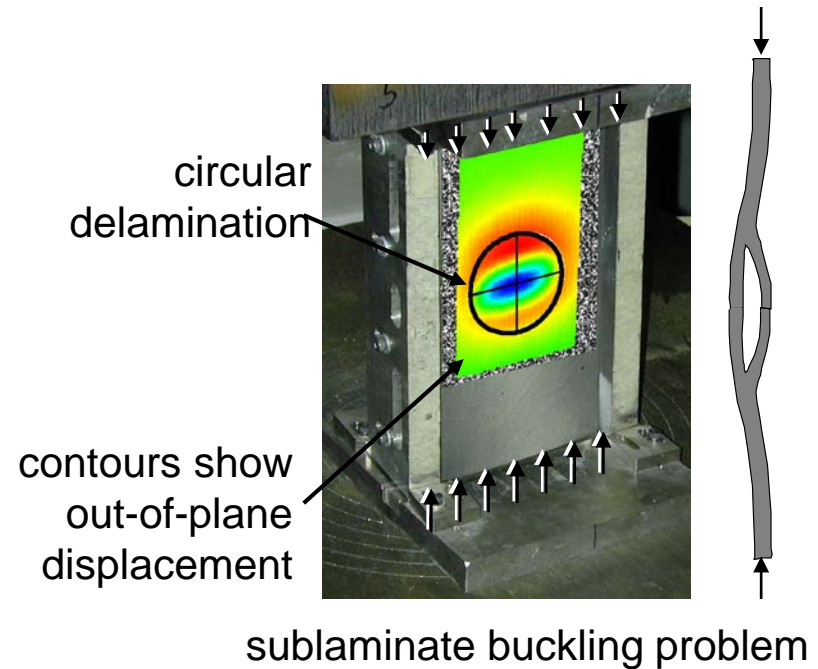
2D Fracture Criterion (only Mode I and Mode II)



B-K Criterion

$$\frac{G_T}{G_{Ic} + (G_{IIc} - G_{Ic}) \left(\frac{G_{II}}{G_T} \right)^\eta} \geq 1$$

3D Problems Contain Mode III



Pure Mode III Testing

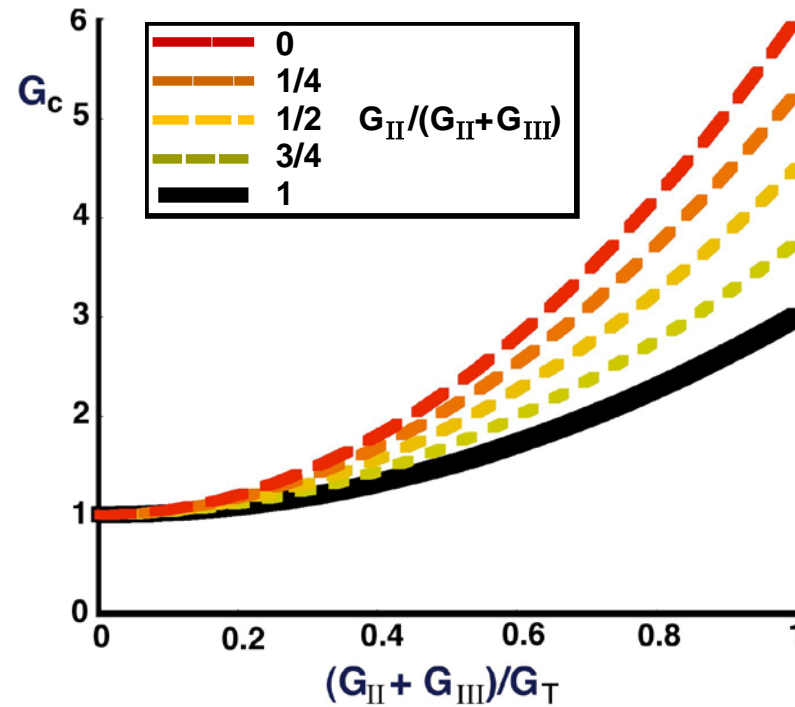
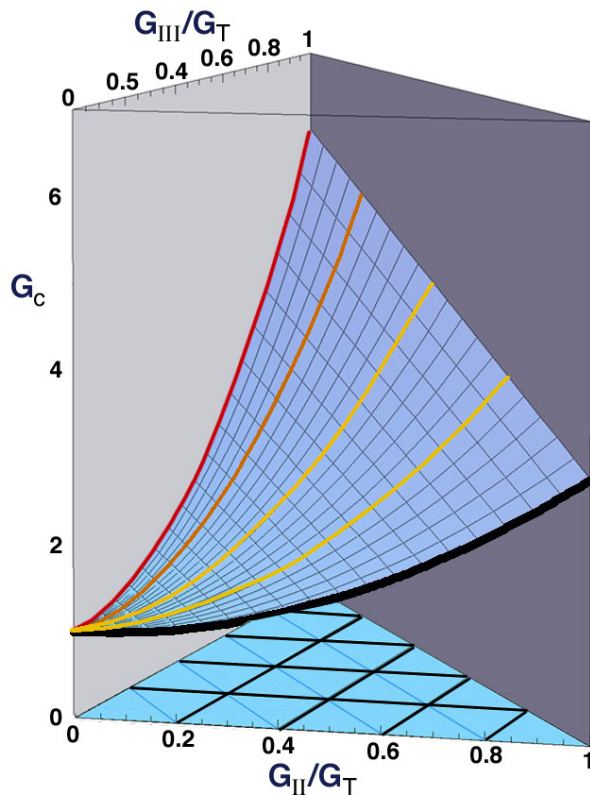
- ECT produces pure mode III data
- G_{IIIc} normally higher than G_{IIc}
- No mixed-mode test with mode III component



edge crack torsion test

Proposed 3D Mixed-Mode Criterion

$$\frac{G_T}{G_{Ic} + (G_{IIc} - G_{Ic}) \left(\frac{G_{II} + G_{III}}{G_T} \right)^\eta + (G_{IIIc} - G_{IIc}) \frac{G_{III}}{G_{II} + G_{III}} \left(\frac{G_{II} + G_{III}}{G_T} \right)^\eta} \geq 1$$



- Mode I-III interaction similar to the measured mode I-II interaction
- Linear interpolation between mode III and mode II



Evolution of Damage Tolerance at NASA Langley (1999-)

Complexity, Computational Expense

Damage Science

Micrographs illustrating damage mechanisms: Stacking Fault, Dislocations, Void Coalescence, and Twinning. Scale bar: 20 μm .

Emerging Continuum Methods

LARC Decohesion Element
(Technology adopted by ABAQUS)

Bilinear Traction-Displacement Law

Mixed-Mode Fracture

FY05 Advances

Delamination growth

Enhanced formulation allows the use of elements up to three times larger than with the classical damage model.

Narrow range vs Wide range of element sizes

$$\frac{G_I}{G_c} + (G_{II} - G_{IIc}) \frac{G_{II} + G_{IIc}}{G_I} + (G_{III} - G_{IIIc}) \frac{G_{III} + G_{IIIc}}{G_I} \geq 1$$

Spin-Offs

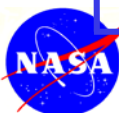
Current State-of-the-Art

Graph showing G_I (in-lb/in²) vs Pressure, P (psi). Parameters: $b=0.7510$, $b=0.6250$, $b=0.5000$.

3D finite element model showing crack growth.

Spin-Offs

Time



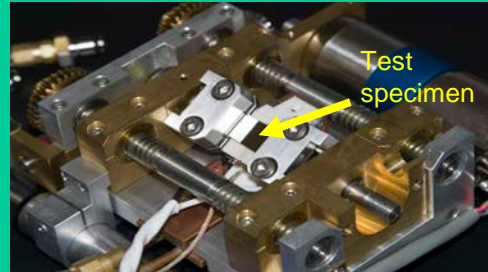
Damage Science

Develop a fundamental understanding of the underlying damage processes that contribute to fracture initiation and propagation

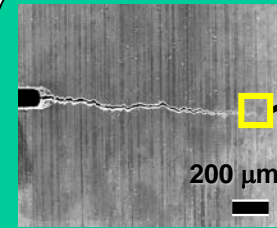
Experimental Damage Science



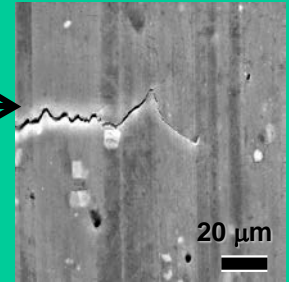
Materials characterization and in-situ mechanical testing with environmental capabilities



In-situ loading frame with heater/cooler and specimen tilt for EBSD analysis



SEM micrograph of fatigue crack emanating from EDM notch

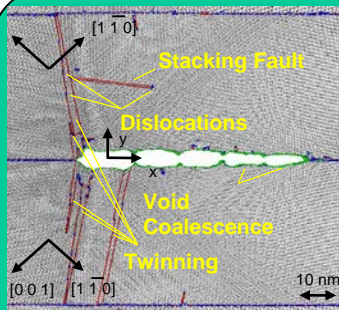


SEM micrograph of fatigue crack tip

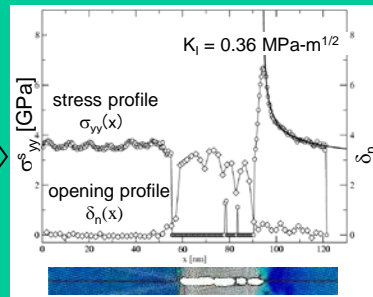
Develop multi-disciplinary Damage Science approach to:

- 1) Characterize material structure and characteristic damage processes,
- 2) Develop multi-scale models to predict damage, and
- 3) Validate models through examination of near-tip damage processes.

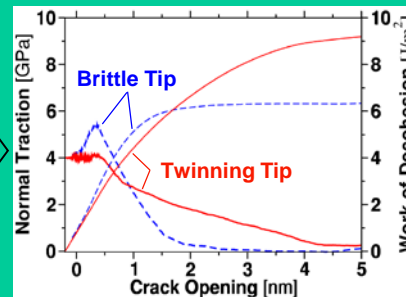
Computational Damage Science



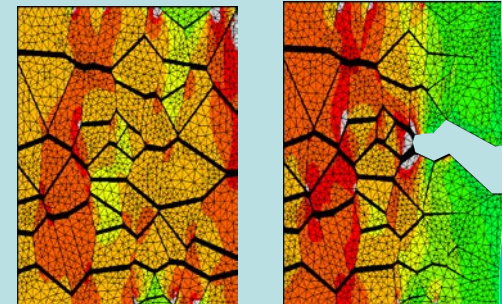
Mechanisms of Nano-crack Propagation



Calculation of Normal Stress and Crack Opening



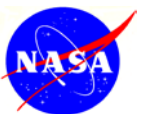
Continuum Representation of Atomistic Behavior



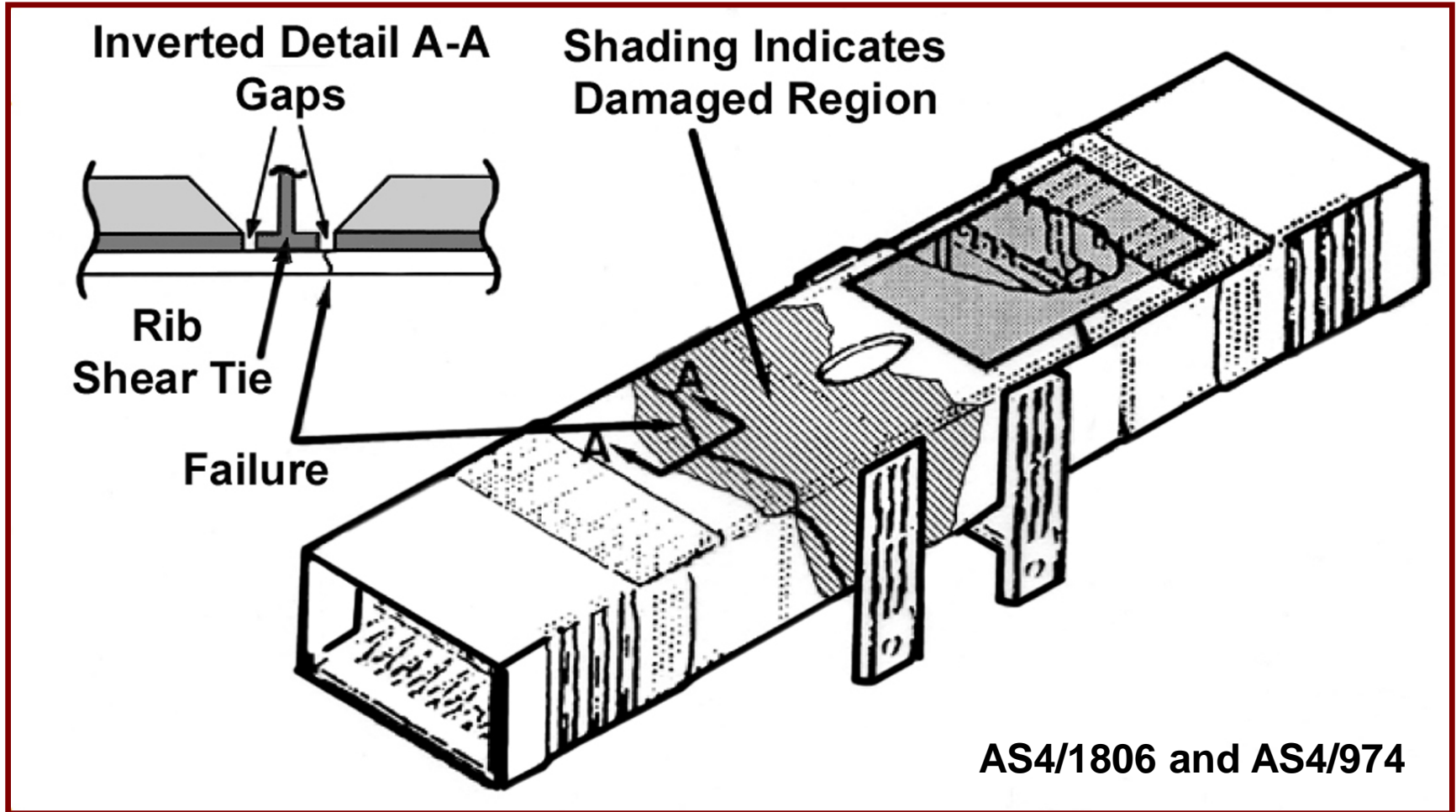
Micro-Scale Crack Growth

Summary

- Damage tolerance of composite wing boxes and full scale wing structures
 - Textile composites
 - Stitching
 - Efficient analysis methods
- SOA analysis demonstrated on
 - X-33 LH2 tank failure
 - AA587 composite lug analysis
- Emerging continuum methods
 - New criteria for interlaminar and intralaminar failure
 - Continuum damage models - Mesh independence
 - Z-pinning
- Damage science to understand failure initiation and growth -
Damage Tolerance



NASA ACT Program – Center Wing Box Test (1991)



- Test Article failed at 83% of DUL under combined bending & torsion
- Unanticipated shear failure mode at out-of-tolerance gap

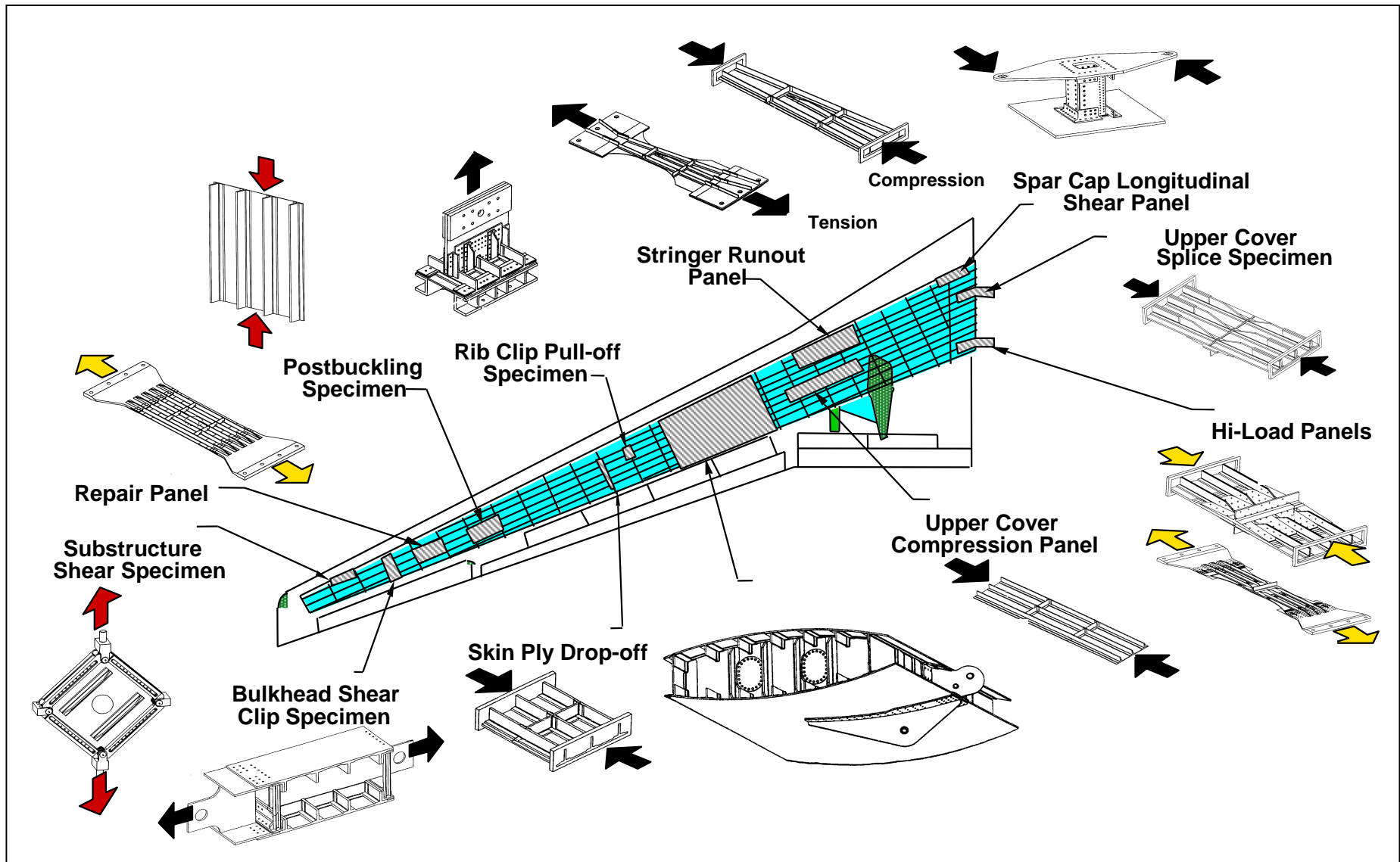
NASA ACT Program – Wing Stub Box Test (1996)



AS4/3501-6 and IM7/3501-6 in textile preform

- **Test article failed at 94% of DUL due to nonvisible impact damage**
- **Compression after impact (CAI) strength allowable did not account for damaged elements (skin/stiffener) interaction**

Building Block Approach – Reliance on Extensive Testing



Progressive Damage Analysis

Modeling Complexities

- Failure of unidirectional and laminated composites (in-situ)
- Material nonlinearity & material degradation laws
- Thermal residual stresses
- Effects of stress gradients & notches
- Size Effects
- Finite Element implementation
- Delamination growth: static & fatigue
- Damage mode interaction
- Stitched composites and textiles

FY04

LaRC04
Failure
Criteria

FY05-06

In-Situ
Strengths

Continuum
Damage Model

Enhanced
Decohesion
Element
&
High-Cycle
Fatigue Model

